Dyes and Pigments 82 (2009) 379–386

Contents lists available at ScienceDirect

Dyes and Pigments

journal homepage: www.elsevier.com/locate/dyepig

The synthesis, characterization and structures of some 4-[((*E*)-1-{2-hydroxy-5-[(*E*)-2-(aryl)-1-diazenyl]phenyl}methylidene)amino]benzoic acid

Tushar S. Basu Baul [a,*], Pradip Das [a], Asit K. Chandra [a], Sivprasad Mitra [a], Simon M. Pyke [b]

[a] Department of Chemistry, North-Eastern Hill University, NEHU Permanent Campus, Umshing, Shillong 793 022, India
[b] School of Chemistry and Physics, Faculty of Sciences, The University of Adelaide, SA 5005, Australia

ARTICLE INFO

Article history:
Received 8 September 2008
Received in revised form
3 February 2009
Accepted 7 February 2009
Available online 19 March 2009

Keywords:
Azo-dyes
4-[((*E*)-1-{2-Hydroxy-5-[(*E*)-2-(aryl)-1-diazenyl]phenyl}methylidene)-amino]benzoic acid
NMR
UV–VIS spectroscopy
DFT calculation
Structures

ABSTRACT

The structures of several azo-benzoic acids, 4-[((*E*)-1-{2-hydroxy-5-[(*E*)-2-(aryl)-1-diazenyl]phenyl}methylidene)amino]benzoic acid along with their precursors 2-hydroxy-5-[(*E*)-(aryldiazenyl)]benzaldehydes were confirmed using ^{1}H, ^{13}C NMR, UV–VIS and IR spectroscopic techniques. UV–VIS absorption spectra were measured in pure organic solvents while complementary spectroscopic experiments using mixed solvent systems as well as in the presence of base were undertaken to characterize the different species present in solution. Both acid–base dissociation and azo–hydrazone tautomerism occurred in solution, with the extent of the individual equilibria being dependent on the solvent composition and/or pH of the medium. Molecular structures and geometries were optimized using the B3LYP density functional theory method employing the 6-31G(d) basis set.

1. Introduction

Salicylaldehyde and their metal complexes are well established [1–3]. More useful organic reagents having the properties of salicylaldehyde together with other desired features, e.g., 5-(arylazo)salicylaldehyde hereafter termed as 2-hydroxy-5-[(*E*)-(aryldiazenyl)]benzaldehydes were also reported. The chemical properties of 2-hydroxy-5-[(*E*)-(aryldiazenyl)]benzaldehyde and its derivatives are of interest due to their coordination capacity with various metal ions such as U(VI) [4], Pd(II) [4], Co(II) [5], Cu(II) [6,7], Ni(II) [8], Mn(II) [9], Sn(II) [10] and Sn(IV) [11]. These reagents were also condensed with anilines which resulted in 5-phenylazosalicylidene aniline and its coordination abilities towards various metals *viz.*, Fe(III), Co(II), Ni(II) and Cu(II) were studied [12]. Recently, a few Cu(II) complexes of some related systems obtained by condensation of 2-hydroxy-5-[(*E*)-(aryldiazenyl)]benzaldehyde with di- and tri-amine have also been reported and the structure of one of the complex was determined using single crystal X-ray crystallography [13].

Recently, we have also investigated related polyaromatic systems, e.g., 2-{(*E*)-4-hydroxy-3-[(*E*)-4-(aryl)iminomethyl]phenyldiazenyl}benzoic acids (**1a**–**d**) (Fig. 1), which contain both azo and imino linkages, owing to possible mesogenic properties. The structures of **1a** [14], **1b** [15] and **1c** [16] were also determined using X-ray crystallography which revealed that the three-ring system assumes an extended conformation, with both outer rings slightly twisted with respect to the central aromatic ring. The carboxylic acid group (in ring C) is coplanar with its parent phenyl ring. The metric parameters within the molecules are similar, except that **1a** exists in a zwitterionic form [14]. Further, these systems were investigated for their coordination behaviour towards organotin(IV) in order to find their possible uses as metallomesogens. The triorganotin(IV) complexes of the general formula $R_3Sn[O_2CC_6H_4\{N{=}N(C_6H_3\text{-}4\text{-}OH(C(H){=}NC_6H_4X\text{-}4)\}\text{-}o]$ ($R = n$Bu and Ph; X = $-CH_3$, –Br, –Cl or $-OCH_3$) also provided structural diversity in the crystalline state and their interesting biological activity [17–20].

Further, 2-hydroxy-5-[(*E*)-(aryldiazenyl)]benzaldehyde (**2a**–**d**) (Fig. 1) can exist in two coloured acid–base forms (neutral and anion), depending on pH of the solution. In addition to acid–base dissociation equilibrium, this group of compounds can exhibit azo–hydrazone tautomerism as exemplified for arylazophenols in Fig. 2(a). Such studies involving substituted azo dyes are directly

* Corresponding author.
E-mail addresses: basubaul@nehu.ac.in, basubaul@hotmail.com (T.S. Basu Baul).

0143-7208/$ – see front matter © 2009 Elsevier Ltd. All rights reserved.
doi:10.1016/j.dyepig.2009.02.012

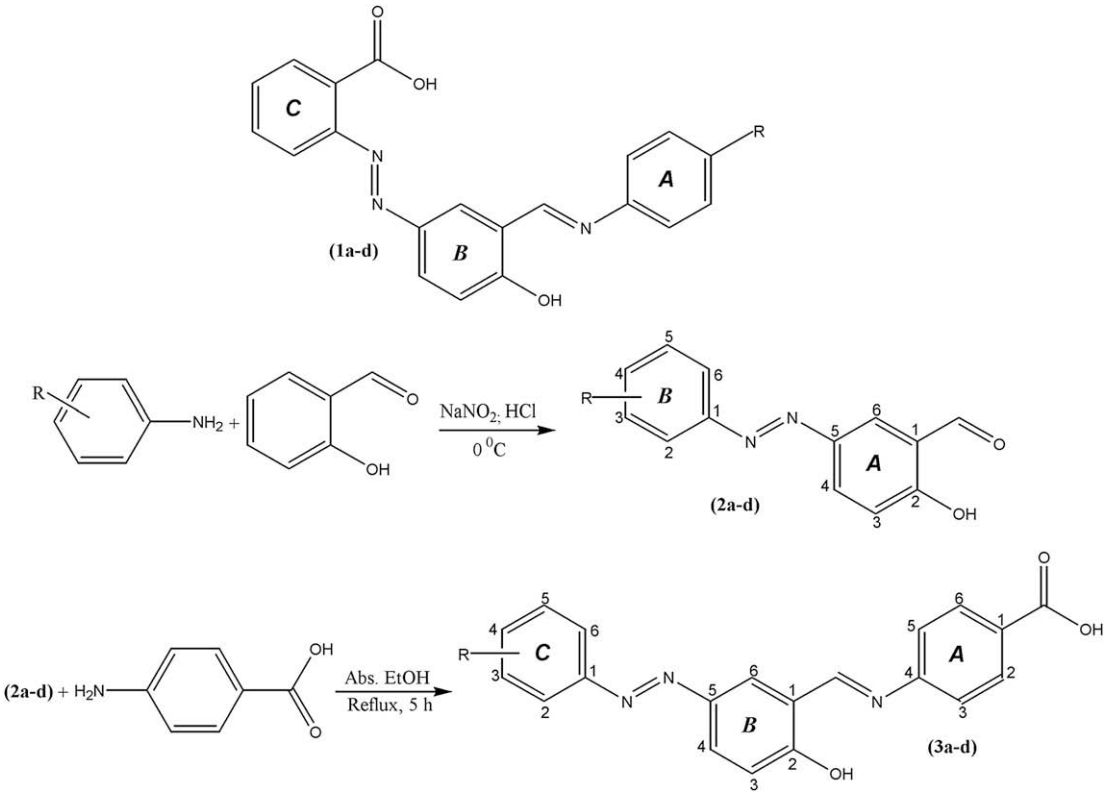

Fig. 1. General structure, reaction schemes and ^{1}H and ^{13}C NMR numbering schemes of the (i) 2-{(*E*)-4-hydroxy-3-[(*E*)-4-(aryl)iminomethyl]phenyldiazenyl}benzoic acid (R = CH_3: **1a**; =Br: **1b**; =Cl: **1c**; =OCH_3: **1d**), (ii) 2-hydroxy-5-[(*E*)-(aryldiazenyl)]benzaldehyde (R = H: **2a**; =2-CH_3: **2b**; =3-CH_3: **2c**; =4-CH_3: **2d**) and (iii) 4-[((*E*)-1-{2-hydroxy-5-[(*E*)-2-(aryl)-1-diazenyl]phenyl}methylidene)amino]benzoic acid (R = H: **3a**; =2-CH_3: **3b**; =3-CH_3: **3c**; =4-CH_3: **3d**). H and H′ refer to the hydroxyl and carboxylic acid protons, respectively.

associated to their frequent use in spectrophotometric determination of metal ions [21]. Furthermore, various salicylideneanilines like **3a–d** (Fig. 1) have attracted considerable attention both experimentally [22–24] and theoretically [25,26] because of their structural simplicity, and also capable of exhibiting intramolecular proton transfer on photoexcitation towards the formation of relatively long lived photochromic product (Fig. 2(b)).

Given the synthetic and structural importance and the potential biological activity of such polyaromatic systems, it is of interest to explore the structure and properties of the analogous systems where now the carboxylic acid group is placed in *p*-position of ring A (see Fig. 1(**3a–d**)). The present contribution details the preparation and spectroscopic characterization of four 4-[((*E*)-1-{2-hydroxy-5-[(*E*)-2-(aryl)-1-diazenyl]phenyl}-methylidene)amino]benzoic acids (Fig. 1(**3a–d**)) along with their four precursors *viz.*, 2-hydroxy-5-[(*E*)-(aryldiazenyl)]benzaldehydes (Fig. 1(**2a–d**)).

2. Experimental

2.1. Materials

Salicylaldehyde (Lancaster) and *p*-aminobenzoic acid (Merck) were used without further purification while the substituted anilines (reagent grade) were distilled prior to use. The solvents used in the reactions were of AR grade and dried using standard procedures, whereas, for UV–VIS experiments spectroscopic grade solvents (>99.9%) were procured from SRL, India and used without any further purification.

2.2. Physical measurements

Carbon, hydrogen and nitrogen analyses were performed with a Perkin Elmer 2400 series II instrument. IR spectra in the range 4000–400 cm^{-1} were obtained on either a BOMEM DA-8 FT-IR or a Perkin Elmer Spectrum BX series FT-IR spectrophotometer with samples investigated as KBr discs. The ^{1}H and ^{13}C NMR spectra of 2-hydroxy-5-[(*E*)-(aryldiazenyl)]benzaldehyde (**2a–d**) and 4-[((*E*)-1-{2-hydroxy-5-[(*E*)-2-(aryl)-1-diazenyl]-phenyl}methylidene)amino]benzoic acid (**3a–d**) were acquired on a Varian INOVA spectrometer operating at 599.91 and 150.85 MHz, respectively. Steady-state absorption spectra were recorded on a Perkin–Elmer model Lambda25 absorption spectrophotometer using quartz cuvettes of 10 mm optical path length received from PerkinElmer, USA. The pH variation experiments were carried out in a Systronics μ-pH system (type 361, resolution 0.01 pH) at constant temperature (293 K). The sample concentration (ca. $8–10 \times 10^{-6}$ mol dm^{-3}) was low enough to avoid any aggregation.

2.3. Synthesis

The compounds 4-[((*E*)-1-{2-hydroxy-5-[(*E*)-2-(aryl)-1-diazenyl]phenyl}-methylidene)amino]benzoic acids (**3a–d**) were synthesized by condensing 2-hydroxy-5-[(*E*)-(aryldiazenyl)]benzaldehydes (**2a–d**) with *p*-aminobenzoic acid.

2.3.1. Preparation of 2-hydroxy-5-[(E)-(aryldiazenyl)]benzaldehyde (*2a–d*)

The compounds, *viz.* 2-hydroxy-5-[(*E*)-phenyldiazenyl]- (**2a**), 2-hydroxy-5-[(*E*)-(2-methylphenyl)diazenyl]- (**2b**), 2-hydroxy-5-

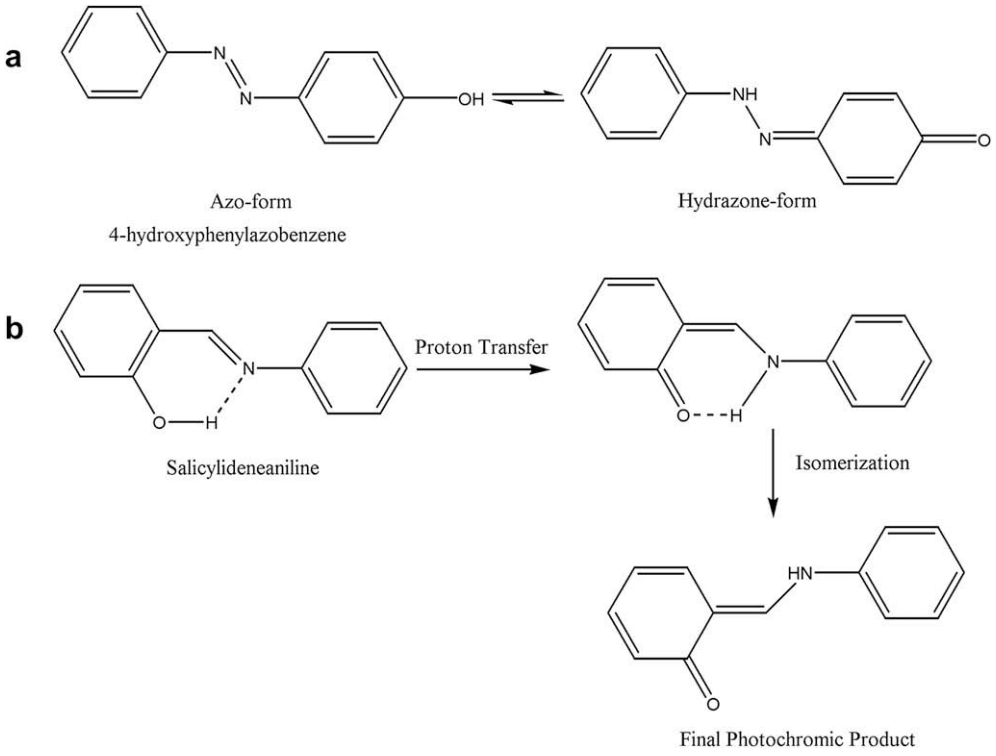

Fig. 2. Various possible structural species in (a) arylazophenols and (b) salicylideneanilines.

[(*E*)-(3-methylphenyl)-diazenyl]- (**2c**) and 2-hydroxy-5-[(*E*)-(4-methylphenyl)diazenyl]benzaldehyde (**2d**) were prepared by reacting appropriate aryldiazonium chloride with salicylaldehyde by previously reported method [27] and the purities were established by their characterization and spectroscopic data which are presented below.

*2.3.1.1. Preparation of 2-hydroxy-5-[(*E*)-phenyldiazenyl]benzaldehyde (**2a**).* Recrystallized from methanol to give yellow microcrystalline product in 60% yield. M.p.: 118–120 °C. Anal. Found. C, 68.92; H, 4.39; N, 12.50. Calc. for $C_{13}H_{10}N_2O_2$: C, 69.02; H, 4.42; N, 12.38%. IR (cm^{-1}): 1666 ν(C═O). ^{1}H NMR ($CDCl_3$); δ_H: 7.12 [d, 8.4 Hz, 1H, A–H3], 7.46 [t, 7.8 Hz, 1H, B–H4], 7.48–7.54 [m, 2H, B–H3/H5], 7.89 [d, 7.8 Hz, 2H, B–H2/H6], 8.17 [dd, 2.4 & 8.4 Hz, 1H, A–H4], 8.20 [d, 2.4 Hz, 1H, A–H6], 10.03 [s, 1H, CHO], 11.32 [s, 1H, OH] ppm. ^{13}C NMR ($CDCl_3$); δ_C: 118.5 [A–C3], 120.3 [A–C1], 122.7 [B–C2/C6], 129.1 [B–C3/C5], 129.3 [A–C6], 130.7 [A–C4], 131.0 [B–C4], 145.9 [A–C5], 152.4 [B–C1], 163.5 [A–C2], 196.5 [CHO] ppm.

*2.3.1.2. Preparation of 2-hydroxy-5-[(*E*)-(2-methylphenyl)l]benzaldehyde (**2b**).* Recrystallized from methanol to give reddish brown microcrystalline product in 70% yield. M.p.: 110–112 °C. Anal. Found. C, 70.12; H, 4.85; N, 11.46. Calc. for $C_{14}H_{12}N_2O_2$: C, 70.00; H, 5.00; N, 11.66%. IR (cm^{-1}): 1659 ν(C═O). ^{1}H NMR ($CDCl_3$); δ_H: 2.72 [s, 3H, CH_3], 7.11 [d, 8.4 Hz, 1H, A–H3], 7.27 [dt, 1.8 & 7.8 Hz, 1H, B–H5], 7.33–7.38 [m, 2H, B–H3/H4], 7.62 [dd, 1.8 & 7.8 Hz, 1H, B–H6], 8.15 [dd, 2.4 & 8.4 Hz, 1H, A–H4], 8.18 [d, 2.4 Hz, 1H, A–H6], 10.02 [s, 1H, CHO], 11.32 [s, 1H, OH] ppm. ^{13}C NMR ($CDCl_3$); δ_C: 15.5 [CH_3], 115.4 [B–C6], 118.5 [A–C3], 120.3 [A–C1], 126.4 [B–C5], 129.7 [B–C6], 130.3 [A–C4], 130.9 [B–C4], 131.5 [B–C3], 138.0 [B–C2], 146.3 [A–C5], 150.4 [B–C1], 163.6 [A–C2], 196.5 [CHO] ppm.

*2.3.1.3. Preparation of 2-hydroxy-5-[(*E*)-(3-methylphenyl)-diazenyl]-benzaldehyde (**2c**).* Recrystallized from ethanol to give brown crystalline product in 78% yield. M.p.: 115–116 °C. Anal. Found. C, 70.02; H, 4.95; N, 11.40. Calc. for $C_{14}H_{12}N_2O_2$: C, 70.00; H, 5.00; N, 11.66%. IR (cm^{-1}): 1659 ν(C═O). ^{1}H NMR ($CDCl_3$); δ_H: 2.46 [s, 3H, CH_3], 7.12 [d, 8.4 Hz, 1H, A–H3], 7.29 [dt, 7.8 & 1.8 Hz, 1H, B–H4], 7.41 [t, 7.8 Hz, 1H, B–H5], 7.70–7.71 [m, 2H, B–H2/6], 8.17 [dd, 2.4 & 8.4 Hz, 1H, A–H4], 8.19 [d, 2.4 Hz, 1H, A–H6], 10.02 [s, 1H, CHO], 11.31 [s, 1H, OH] ppm. ^{13}C NMR ($CDCl_3$); δ_C: 21.3 [CH_3], 118.5 [A–C3], 120.3 [A–C1], 120.4 [B–C6], 122.9 [B–C2], 128.9 [B–C5], 129.2 [A–C6], 130.7 [A–C4], 131.8 [B–C4], 139.1 [A–C3], 145.9 [A–C5], 152.5 [B–C1], 163.7 [A–C2], 196.5 [CHO] ppm.

*2.3.1.4. Preparation of 2-hydroxy-5-[(*E*)-(4-methylphenyl)-diazenyl]benzaldehyde (**2d**).* Recrystallized from methanol to give yellow microcrystalline product in 79% yield. M.p.: 128–130 °C. Anal. Found. C, 69.92; H, 4.82; N, 11.56. Calc. for $C_{14}H_{12}N_2O_2$: C, 70.00; H, 5.00; N, 11.66%. IR (cm^{-1}): 1659 ν(C═O). ^{1}H NMR ($CDCl_3$); δ_H: 2.44 [s, 3H, CH_3], 7.11 [d, 8.4 Hz, 1H, A–H3], 7.31 [AA′ portion of AA′XX′, 2H, B–H3/H5], 7.81 [XX′ portion of AA′XX′, 2H, B–H2/H6], 8.16 [dd, 8.4 & 2.4 Hz, 1H, A–H4], 8.17 [d, 2.4 Hz, 1H, A–H6], 10.02 [s, 1H, CHO], 11.3 [s, 1H, OH] ppm. ^{13}C NMR ($CDCl_3$); δ_C: 21.5 [CH_3], 118.5 [A–C3], 120.3 [A–C1], 122.7 [B–C2/C6], 129.0 [A–C6], 129.8 [B–C3/C5], 130.7 [A–C4], 141.7 [B–C4], 145.9 [A–C5], 150.5 [B–C1], 163.5 [A–C2], 196.6 [CHO] ppm.

*2.3.2. Preparation of 4-[((*E*)-1-{2-hydroxy-5-[(*E*)-2-(aryl)-1-diazenyl]phenyl}methylidene)amino]benzoic acid (**3a**–**d**)*

A typical procedure is described below.

*2.3.2.1. Preparation of 4-[((*E*)-1-{2-hydroxy-5-[(*E*)-2-phenyl-1-diazenyl]phenyl}methylidene)amino]benzoic acid (**3a**).* An equimolar amount of *p*-aminobenzoic acid (0.61 g, 4.42 mmol) in hot ethanol (20 ml) was added slowly to a hot ethanol solution (50 ml) containing 2-hydroxy-5-[(*E*)-phenyldiazenyl]benzaldehyde (**2a**) (1.00 g, 4.42 mmol) and the reaction mixture was refluxed for 5 h. The water formed during the reaction was removed using a Dean–Stark apparatus. The reaction mixture was concentrated to half of

the initial solvent volume on a hot plate, cooled to room temperature whereupon a reddish orange solid precipitated. The precipitate was filtered, washed with hexane (3 × 5 ml) and then dried in air. The crude product was washed with hot hexane to remove any tarry materials. Yield: 1.12 g, 69.5%. M.p.: 264–266 °C. Anal. Found. C, 69.50; H, 4.32; N, 11.98. Calc. for $C_{20}H_{15}N_3O_3$: C, 69.56; H, 4.38; N, 12.17%. IR (cm^{-1}): 1699 ν(C═O); 1622 ν(C═N). ^{1}H NMR (DMSO-d_6); δ_H: 7.15 [d, 9.0 Hz, 1H, B–H3], 7.50–7.54 [m, 3H, A–H3/H5 & C–H4], 7.56 [m, 2H, C–H3/H5], 7.84 [m, 2H, C–H2/H6], 8.02 [dd, 9.0 & 2.4 Hz, 1H, B–H4], 8.03 [XX′ portion of AA′XX′, 2H, A–H2/H6], 8.31 [d, 2.4 Hz, 1H, B–H6], 9.14 [s, 1H, CHN], 12.85 [br s, 1H, OH], 13.31 [br s, 1H, OH] ppm. ^{13}C NMR (DMSO-d_6); δ_C: 117.9 [B–C3], 118.4 [B–C1], 121.5 [A–C3/C5], 122.3 [C–C2], 127.5 [B–C6], 127.6 [B–C5], 129.1 [A–C1], 129.4 [C–C3], 130.7 [A–C2/C6], 130.9 [C–C4], 144.8 [B–C5], 151.6 [A–C4], 151.9 [C–C1], 163.4 [B–C2], 163.9 [CHN], 168.2 [CO_2H] ppm.

The other 4-[((*E*)-1-{2-hydroxy-5-[(*E*)-2-(aryl)-1-diazenyl]phenyl}methylidene)amino]benzoic acids (**3b**–**c**) were prepared analogously by reacting appropriate 2-hydroxy-5-[(*E*)-(aryldiazenyl)]benzaldehyde (**2b**–**d**) and *p*-aminobenzoic acid. The characterization and spectroscopic data are presented below.

*2.3.2.2. Preparation of 4-[((*E*)-1-{2-hydroxy-5-[(*E*)-2-(2-methylphenyl)-1-diazenyl]phenyl}methylidene)amino]benzoic acid (**3b**).* Orange-red precipitate in 79% yield. M.p.: 248–250 °C. Anal. Found. 69.95; H, 4.65; N, 11.65. Calc. for $C_{21}H_{17}N_3O_3$: C, 70.18; H, 4.77; N, 11.69%. IR (cm^{-1}): 1692 ν(C═O); 1623 ν(C═N). ^{1}H NMR (DMSO-d_6); δ_H: 2.67 [s, 3H, CH_3], 7.16 [d, 8.4 Hz, 1H, B–H3], 7.28–7.32 [m, 1H, C–H5], 7.38–7.42 [m, 2H, C–H3/H4], 7.53 [AA′ portion of AA′XX′, 2H, A–H3/H5], 7.55 [d, 7.8 Hz, 1H, C–H6], 8.01 [dd, 8.4 & 2.4 Hz, 1H, B–H4], 8.03 [XX′ portion of AA′XX′, 2H, A–H2/H6], 8.32 [d, 2.4 Hz, 1H, B–H6], 9.16 [s, 1H, CHN], 12.75 [br s, 1H, OH], 13.37 [br s, 1H, OH] ppm. ^{13}C NMR (DMSO-d_6); δ_C: 17.0 [CH_3], 115.0 [C–C6], 118.4 [B–C3], 119.3 [B–C1], 121.6 [A–C3/C5], 126.5 [C–C5], 127.3 [B–C4], 129.1 [A–C1], 128.1 [B–C6], 130.7 [A–C2/C6], 130.8 [C–C4], 131.3 [C–C3], 137.1 [C–C2], 145.3 [B–C5], 149.8 [C–C1], 151.5 [A–C4], 163.2 [B–C2], 164.1 [CHN], 166.8 [CO_2H] ppm.

*2.3.2.3. Preparation of 4-[((*E*)-1-{2-hydroxy-5-[(*E*)-2-(3-methylphenyl)-1-diazenyl]phenyl}methylidene)amino]benzoic acid (**3c**).* Brick-red precipitate in 81% yield. M.p.: 262–264 °C. Anal. Found. 69.90; H, 4.70; N, 11.60. Calc. for $C_{21}H_{17}N_3O_3$: C, 70.18; H, 4.77; N, 11.69%. IR (cm^{-1}): 1679 ν(C═O); 1622 ν(C═N). ^{1}H NMR (DMSO-d_6); δ_H: 2.40 [s, 3H, CH_3], 7.16 [dd, 9.0 Hz, 1H, B–H3], 7.38 [d, 8.4 Hz, 1H, C–H4], 7.45 [t, 8.4 Hz, 1H, C–H5], 7.52 [AA′ portion of AA′XX′, 2H, A–H3/H5], 7.65–7.67 [m, 2H, C–H2/H6], 8.00 [dd, 9.0 & 2.4 Hz, 1H, B–H4], 8.03 [XX′ portion of AA′XX′, 2H, A–H2/H6], 8.31 [d, 2.4 Hz, 1H, B–H6], 9.14 [s, 1H, CHN], 12.71 [br s, 1H, OH], 13.30 [br s, 1H, OH] ppm. ^{13}C NMR (DMSO-d_6); δ_C: 20.8 [CH_3], 117.9 [B–C3], 119.4 [B–C1], 119.9 [C–C6], 121.5 [A–C3/C5], 122.4 [C–C2], 127.4 [B–C4], 127.5 [B–C6], 129.1 [C–C5], 129.2 [A–C1], 130.7 [A–C2/C6], 131.6 [C–C4], 138.8 [C–C3], 144.8 [B–C5], 151.6 [A–C4], 151.9 [C–C1], 163.3 [B–C2], 163.8 [CHN], 167.4 [CO_2H] ppm.

*2.3.2.4. Preparation of 4-[((*E*)-1-{2-hydroxy-5-[(*E*)-2-(4-methylphenyl)-1-diazenyl]phenyl}methylidene)amino]benzoic acid (**3d**).* Dark red precipitate in 78% yield. M.p.: 275–277 °C. Anal. Found. C, 70.09; H, 4.60; N, 11.63. Calc. for $C_{21}H_{17}N_3O_3$: C, 70.18; H, 4.77; N, 11.69%. IR (cm^{-1}): 1699 ν(C═O); 1622 ν(C═N). ^{1}H NMR (DMSO-d_6); δ_H: 2.39 [s, 3H, CH_3], 7.16 [d, 9.0 Hz, 1H, B–H3], 7.38 [AA′ portion of AA′XX′, 2H, C–H3/H5], 7.53 [AA′ portion of AA′XX′, 2H, A–H3/H5], 7.76 [XX′ portion of AA′XX′, 2H, C–H2/H6], 8.00 [dd, 9.0 & 2.4 Hz, 1H, B–H4], 8.03 [XX′ portion of AA′XX′, 2H, A–H2/H6], 8.30 [d, 2.4 Hz, 1H, B–H6], 9.15 [s, 1H, CHN], 12.55 [br s, 1H, OH], 13.29 [br s, 1H, OH] ppm. ^{13}C NMR (DMSO-d_6); δ_C: 20.9 [CH_3], 117.9 [B–C3], 119.4 [B–C1], 121.5 [A–C3/C5], 122.2 [C–C2], 127.3 [B–C6], 127.6 [B–C4], 129.0 [A–C1], 129.9 [C–C3], 130.7 [A–C2/C6], 141.1 [C–C4], 144.8 [B–C5], 149.9 [C–C1], 151.7 [A–C4], 163.1 [B–C2], 163.9 [CHN], 166.8 [CO_2H] ppm.

(Note: The compounds (**3a**–**d**) could not be recrystallized owing to limited solubility. The purity of the product was judged on the basis of the analytical and NMR spectroscopic data which provided satisfactory results.)

3. Results and discussion

The 2-hydroxy-5-[(*E*)-(aryldiazenyl)]benzaldehydes (**2a**–**d**) were prepared by following diazo-coupling reaction between the appropriate aryldiazonium chloride with salicylaldehyde in alkaline medium under cold conditions [27]. On the other hand, 4-[((*E*)-1-{2-hydroxy-5-[(*E*)-2-(aryl)-1-diazenyl]phenyl}methylidene)amino]benzoic acids (**3a**–**d**) were prepared by condensation of equimolar amounts of *p*-aminobenzoic acid with appropriate benzaldehydes (**2a**–**d**) in anhydrous ethanol at reflux temperature. The compound frameworks are shown in Fig. 1 while their synthetic details and spectroscopic data are presented in Section 2.3.

3.1. NMR spectroscopy

Characterization of compounds (**2a**–**d** in $CDCl_3$ and **3a**–**d** in DMSO-d_6) was performed by ^{1}H, ^{13}C NMR. A combination of 1D ^{1}H, ^{13}C (proton decoupled and DEPT) and 2D ^{1}H–^{13}C correlated spectroscopy (COSY), heteronuclear single-quantum correlation (HSQC) and heteronuclear multiple-bond connectivity (HMBC) experiments performed by gradient coherence allowed complete assignment of all ^{1}H and ^{13}C resonances. These data are summarized in Section 2.3 which supported the formulation of the compounds.

3.2. UV–VIS spectroscopy

The identification of several species present in the solution of compounds **2a**–**d** and **3a**–**d** was done by UV–VIS absorption spectroscopy under different experimental conditions. Summary of the results are given in Table 1.

The absorption spectra of compounds **3a**–**d** show a single absorption peak at ~338 nm in both carbon tetrachloride and acetonitrile solutions; whereas, compounds **2a**–**d** show one absorption peak in the similar region along with a shoulder at 435–445 nm region. However, in methanol solution all the compounds (**2a**–**d** and **3a**–**d**) show a single absorption in 335–350 nm regions. In contrast, in DMSO solution all the compounds show the principle absorption peak at ~345 nm along with a red shifted shoulder in the 450–470 nm regions. In methanol, the main absorption peak of

Table 1
Summary of the UV–VIS results for compounds (**2a**–**d** and **3a**–**d**) in some representative solvents.[a]

Compound	λ_{max}			
	CCl_4	CH_3CN	DMSO	CH_3OH
2a	334, 445 (sh)	330, 440 (sh)	342, 450 (sh)	345
2b	339, 445 (sh)	335, 435 (sh)	346, 450 (sh)	352
2c	336, 445 (sh)	333, 435 (sh)	346, 450 (sh)	348
2d	338, 445 (sh)	335, 438 (sh)	347, 450(sh)	346
3a	333	333	345, 470 (sh)	335
3b	338	336	334, 468 (sh)	338
3c	338	334	345, 463 (sh)	339
3d	333	337	353, 462 (sh)	337

[a] λ_{max} indicates the wavelength of maximum absorption in nm; (sh) indicates a shoulder.

2a–**d** was found to be shifted about 5–15 nm when compared with other solvent systems (Table 1). This could be due to the stronger hydrogen bonding ability of methanol with the studied molecules. The facile formation of intermolecular hydrogen bonded complex with solvent stabilizes the charge-transfer excited state and consequently, the absorption spectrum is seen to shift towards the long wavelength region [28]. The principal absorption band at 340 nm region for all the compounds having large molar absorptivities ($\varepsilon \approx 0.5$–1.5×10^5 dm^3 mol^{-1} cm^{-1}) is due to the $\pi\pi^*$ transition of the primary azo structure (see Section 3.3). The spectra are shown in Fig. 3 for compound **2c**, but such spectral patterns apply equally well to others and it is apparent that varying the substituents in the compounds has an insignificant influence on the overall spectral pattern.

Multiple absorption peaks (or shoulders) in the spectra of the hydroxyazo-compounds may be observed due to azo ↔ hydrazone tautomerism [29,30]. This equilibrium is known to be favourable in alcoholic solvents. Dissociation of hydroxyl proton in various solvents results in the formation of anion (as shown in Fig. 6c) which may also show an additional absorption peak (or shoulder) depending upon the extent of dissociation [31]. The longer wavelength absorption band for compounds **2a**–**d** can be assumed to be originated from the proton dissociated anionic structure (see Section 3.3). This is further confirmed by measuring the absorption properties in basic solutions. On addition of alkali, the intensity of 335 nm band for **2b** in acetonitrile decreases with a concomitant increase in 435 nm peak intensity. The presence of a clear isosbestic point at ~361 nm further confirms the acid–base equilibrium (Fig. 4). Similar results were also observed for other systems (**2a**, **c**, **d**) and (**3a**–**d**).

The absorption spectra of **2a**–**d** in methanol are notably different from that in other solvents in two ways (Fig. 3): (a) the main absorption band is substantially broad (~9000 cm^{-1} for compound **2c** in methanol compared to ~6000 cm^{-1} in acetonitrile and ~6600 cm^{-1} in DMSO); and (b) the absence of any anionic band at 435–445 nm region. The width of a spectral band can be associated with the presence of multiple species with similar energy parameters. It is well known that the formation of hydrazone tautomer is generally favoured in alcoholic solvents for *p*-hydroxy(phenyl)azo compounds. The large spectral width of the compounds in methanol can be assumed to be associated with the

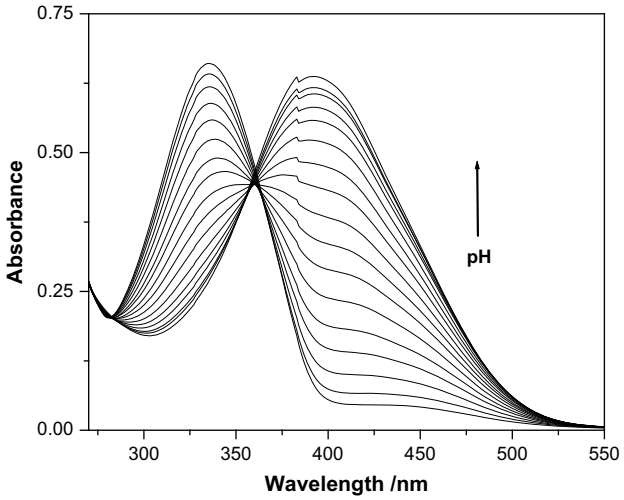

Fig. 4. Variation of UV–VIS spectra of **2b** in acetonitrile with increasing pH of the solutions. The arrow direction indicates the increase in pH from 6.8 to 9.9.

development of appreciable azo ↔ hydrazone tautomerism equilibria compared with other solvents. It is to be mentioned here that no additional/new peak is observed for the hydrazone conformer in methanol (Table 1). This may be due to the very weak transition intensity of the hydrazone conformer so that the absorption of this species is buried under relatively intense spectral band corresponding to the azo structure. Instead, the broadening of the main absorption band was assigned to the presence of multiple species (e.g., hydrazone tautomer along with the azo form) in alcoholic solvents. Furthermore, the fraction of the anionic conformer in this solvent is rather low as evidenced by the absence of longer wavelength absorption band.

However, in the mixed solvent (e.g., **2c** in methanol/acetonitrile mixture), the decrease in alcohol content induces reduction in the band width of the primary form favouring the proton dissociation equilibrium between the normal and anion structure to be established and, consequently, the longer wavelength anionic absorption disappears with methanol content of 30% (v/v) or above in the mixture (Fig. 5). The increased spectral width in alcoholic solvent is

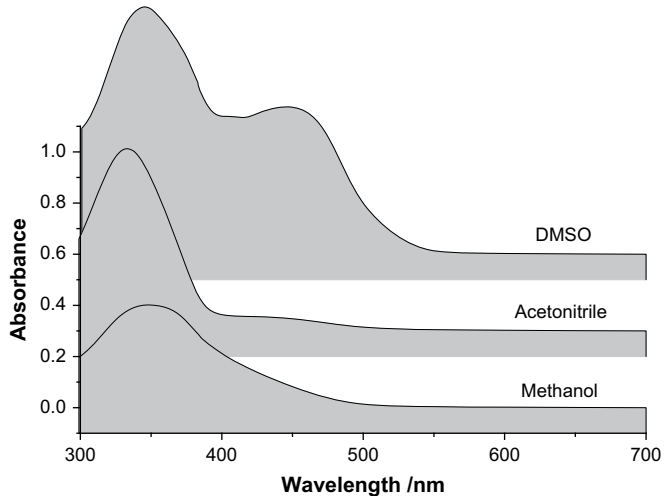

Fig. 3. UV–VIS spectra of **2c** in different solvents. The spectra are scaled vertically for clarity.

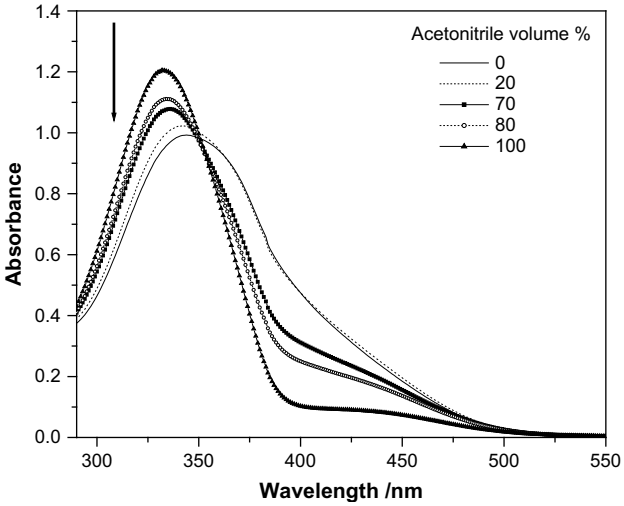

Fig. 5. Variation of UV–VIS spectra of **2c** in acetonitrile/methanol solvent mixture. The proportion of methanol content in the mixture increases along the arrow direction.

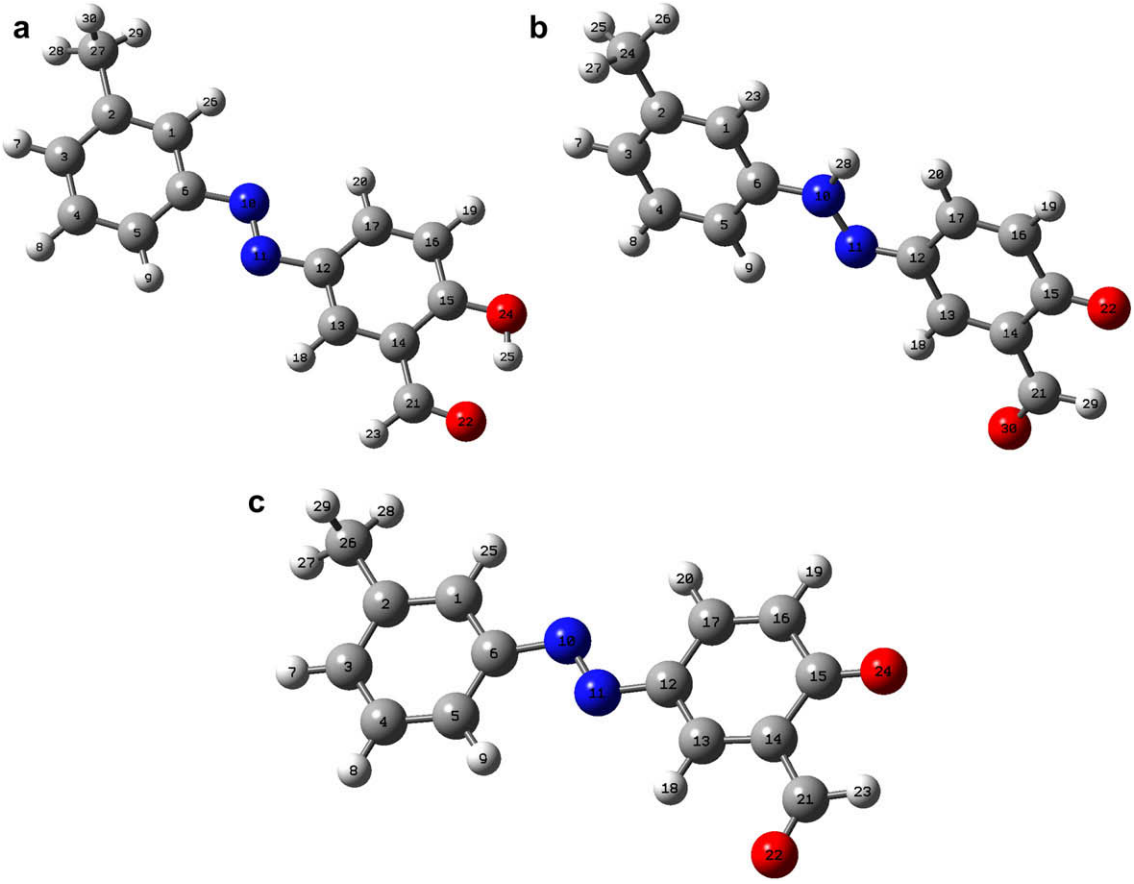

Fig. 6. The structure of compound **2c** (a) azo form (b) hydrazone form (c) anionic form obtained after full geometry optimization at DFT level (refer to the Supplementary materials for the structures of other compounds (**2a**, **b** and **d**)).

due to the coexistence of both hydrazone and azo tautomers (see Section 2.3).

3.3. Quantum chemical calculations

The geometries of the compounds (**2a–d** and **3a–d**) were fully optimized using the B3LYP [32] density functional theory (DFT) method with the 6-31G(d) basis set. Harmonic frequency calculations were performed at all the stationary points to characterize its nature and to ensure that the optimized structure corresponds to a global minimum. The calculated infrared frequency values are then scaled by a factor of 0.9623 [33] to compare with experimental infrared data since the experimental frequency values involve a harmonic term whereas the calculated frequency values are derived from harmonic frequencies. Two representative structures e.g., **2c** (azo form, hydrazone form and anionic form) and **3b** are only shown in Figs. 6(a–c) and 7, respectively, since there is not much differences between this structure and other structures in each of the series of compounds (**2a–d** and **3a–d**). The optimized geometric parameters for the azo conformers of compounds (**2a–d** and **3a–d**) are listed in Tables 2 and 3.

The basic structural framework that contains two phenyl rings and the N=N linkage is found to be planar in the optimized structures of compounds (**2a–d**). This allows the π-electron conjugation to extend throughout the two phenyl rings. The bond lengths and angles are found to be rather insensitive to the position of methyl substitution. The O(22)···H(25) distance in the optimized structures of compounds (**2a–d**) amounts to 174 pm. This distance is much shorter than the sum of van der Waals radii of oxygen (152 pm) and hydrogen (120 pm) atoms. It indicates the presence of hydrogen bonding interactions between the O–H bond and the oxygen atom of the C(H)O group. It is difficult to determine precisely the O–H stretching frequency for the hydrogen bonded O–H, because of the well-known broadening effect. However, our calculated vibrational frequency for each of the structures shows a large red shift of this stretching frequency. For example, the O–H stretching frequency in compound **2c** appears at 3191 cm^{-1}; which is 466 cm^{-1} lower than the experimental value (3657 cm^{-1}) of the O–H stretching frequency in phenol [34]. Similar red shift in O–H stretching frequency has also been observed for other compounds (**2a**, **b** and **d**). This hydrogen bonding will certainly affect the acidity of the O–H bond and the basicity of oxygen atom, which in turn might affect the reactivity. The C=O stretching vibrational frequency (1670 cm^{-1}) is found to be almost unchanged in compounds **2a–d**. Similar observation was also made from the experimental infrared spectra of these compounds. The calculated C=O stretching frequency (1670 cm^{-1}) is in very good agreement with the experimental value of 1667 cm^{-1}.

The optimized geometrical parameters for compounds **3a–c** show that bond lengths, bond angles and torsion angles remain virtually unchanged. Hence it may be inferred that neither substitution of H-atom of the terminal phenyl ring by methyl group, nor the site of substitution has any effect on the structure of these compounds. The noticeable structural change that occurs from the structure of compounds **2a–d** to the corresponding compounds **3a–d** is the loss of planarity. In the structures of compounds **3a–d**, the precursor part of the molecule remains planar, but the phenyl ring containing the carboxylic (–COOH) group does not belong to the same plain. This has been reflected from the C(22)–N(23)–C(27)–C(28) torsion angle and the –COOH containing phenyl ring is tilted by almost 36° from the

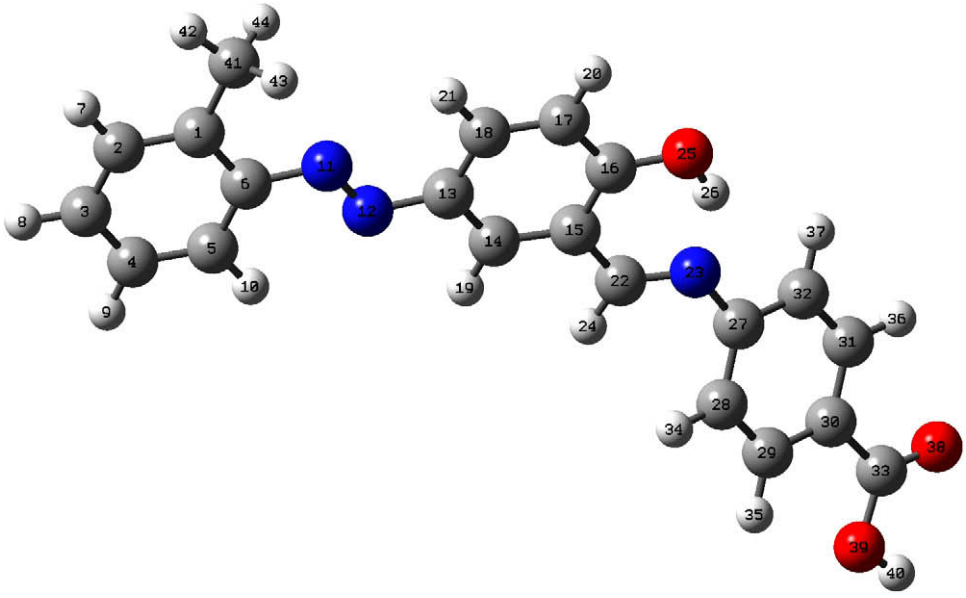

Fig. 7. The structure of compound **3b** obtained after full geometry optimization at DFT level (refer to the Supplementary materials for the structures of other compounds (**3a**, **c** and **d**)).

plain containing the precursor part of the moiety. The optimized structures of these compounds (**3a**–**d**) indicate the formation of a strong O(25)–H(26)···N(23) hydrogen bond. The N(23)···H(26) distance is calculated to be around 174 pm, which is much shorter than the sum of the van der Waals radii of nitrogen (155 pm) and hydrogen (120 pm). Moreover, the red shift of O–H stretching frequency provides further indication of this hydrogen bonding.

To verify the spectral assignments made in the previous section, the transition energies for several conformers were estimated by time dependent density functional theory (TDDFT) using

Table 2
Selected bond lengths, bond angles and torsion angles for optimized structures (B3LYP/6-31G(d)) of azo conformer of compounds (**2a**–**d**).[a]

Bond lengths (pm)/angles (°)	2a	2b	2c	2d
C(15)–O(24)	133.61	133.64	133.64	133.65
O(24)–H(25)	99.33	99.32	99.31	99.32
N(10)–N(11)	126.22	126.28	126.22	126.30
C(21)–O(22)	123.38	123.38	123.38	123.40
O(22)–H(25)	174.17	174.27	174.37	174.13
C(2)–C(27)	–	151.01	151.13	150.96
O(22)–C(21)–H(23)	119.58	119.58	119.57	119.56
C(14)–C(15)–O(24)	121.91	121.93	121.92	121.92
C(15)–O(24)–H(25)	107.23	107.25	107.24	107.19
O(24)–C(15)–C(16)	118.71	118.73	118.71	118.74
C(13)–C(12)–N(11)	116.18	116.07	116.14	116.25
C(17)–C(12)–N(11)	124.94	125.13	125.0	124.92
N(11)–N(10)–C(6)	114.90	115.14	114.85	115.01
N(10)–C(6)–C(5)	124.81	123.52	124.79	125.06
N(10)–C(6)–C(1)	115.34	115.91	115.22	115.64
C(5)–C(6)–C(1)	119.84	120.57	119.99	119.30
C(3)–C(2)–C(27)[b]	–	120.57	121.08	121.31
C(1)–C(2)–C(27)[c]	–	121.49	120.89	120.47
C(15)–C(14)–C(21)–O(22)	0.0	0.0	0.0	0.0
C(14)–C(15)–O(24)–H(25)	0.0	0.0	0.0	0.0
N(10)–N(11)–C(12)–C(17)	0.0	0.01	0.02	0.0
C(6)–N(10)–N(11)–C(12)	180	180	180	180

[a] Refer to Fig. 6 for atomic numbering scheme.
[b] The corresponding bond angles are C(6)–C(1)–C(27) and C(4)–C(3)–C(27) for **2b** and **d**, respectively.
[c] The corresponding bond angles are C(6)–C(1)–C(27) and C(2)–C(3)–C(27) for **2b** and **d**, respectively.

Table 3
Selected bond lengths, bond angles and torsion angles for optimized structures (B3LYP/6-31G(d)) of azo conformer of compounds (**3a**–**d**).[a]

Bond lengths (pm)/angles (°)	3a	3b	3c	3d
C(33)–O(38)	121.53	121.53	121.53	121.54
C(33)–O(39)	135.93	135.93	135.94	135.94
O(39)–H(40)	97.50	97.50	97.49	97.49
C(16)–O(25)	133.56	133.59	133.59	133.62
O(25)–H(26)	99.99	99.99	99.98	99.96
N(11)–N(12)	126.26	126.32	126.26	126.33
C(22)–N(23)	129.35	129.35	129.35	129.36
N(23)–H(26)	174.33	174.31	174.36	174.45
C(1)–C(41)	–	151.00	151.14	150.97
O(38)–H(40)	226.53	226.52	226.51	226.50
C(33)–O(39)–H(40)	105.55	105.54	105.54	105.53
O(38)–C(33)–O(39)	121.93	121.93	121.93	121.92
O(38)–C(33)–C(30)	124.99	124.99	125.0	125.02
C(33)–C(30)–C(31)	118.12	118.12	118.13	118.15
C(28)–C(27)–N(23)	123.05	123.07	123.01	122.99
N(23)–C(22)–H(24)	121.20	121.21	121.18	121.17
C(15)–C(16)–O(25)	122.16	122.18	122.16	122.17
C(16)–O(25)–H(26)	107.47	107.48	107.47	107.48
O(25)–C(16)–C(17)	118.37	118.38	118.38	118.37
C(14)–C(13)–N(12)	116.02	115.94	116.02	116.06
C(18)–C(13)–N(12)	125.04	125.18	125.05	125.03
N(12)–N(11)–C(6)	114.84	115.13	114.83	114.92
N(11)–C(6)–C(5)	124.84	123.56	124.86	125.04
N(11)–C(6)–C(1)	115.36	115.90	115.21	115.70
C(5)–C(6)–C(1)	119.80	120.54	119.93	119.25
C(2)–C(1)–C(41)[b]	–	120.61	121.11	120.50
C(6)–C(1)–C(41)[c]	–	121.41	120.87	121.33
O(38)–C(33)–O(39)–H(40)	0.0	0.0	0.0	0.10
C(16)C–(15)–C(22)–N(23)	−0.26	−0.27	−0.35	−0.40
C(15)–C(16)–O(25)–H(26)	0.41	0.48	0.35	0.32
N(11)–N(12)–C(13)–C(18)	1.17	1.51	−0.11	−0.47
C(6)–N(11)–N(12)–C(13)	179.96	179.68	180.0	180.0
C(14)–C(15)–C(22)–N(23)	179.48	179.45	179.56	179.59
C(15)–C(22)–N(23)–C(27)	177.48	177.45	177.20	177.08
C(22)–N(23)–C(27)–C(28)	−35.79	−35.51	−35.93	−36.18
N(23)–C(27)–C(28)–C(29)	179.36	179.47	179.31	179.24
C(29)–C(30)–C(33)–O(39)	0.37	0.35	0.39	0.43

[a] Refer to Fig. 6 for atomic numbering scheme.
[b] The corresponding bond angles are C(3)–C(2)–C(41) and C(4)–C(3)–C(41) for **3c** and **d**, respectively.
[c] The corresponding bond angles are C(1)–C(2)–C(41) and C(2)–C(3)–C(41) for **3c** and **d**, respectively.

6-311G(d,p) basis set. The calculated results indicate $\pi \rightarrow \pi^*$ transition for all the structures and agree reasonably well with the experimentally measured spectral data mentioned in Table 1. For example, the calculated gas phase transitions for azo, hydrazone and anionic forms of compound **2b** appear at 362, 408 and 418 nm, respectively. This is in good agreement with the experimental data obtained from UV–VIS results *viz.*, 340, 410 and 420–440 nm, respectively, in acetonitrile solution. Close agreement of the calculated and experimentally obtained absorption maxima as well as infrared frequencies further substantiates the validity of the structures obtained from DFT calculations.

In conclusion, the synthesis, analytical characterization, solution phase spectroscopic properties for a series of 2-hydroxy-5-[(*E*)-(aryldiazenyl)]benzaldehydes (**2a**–**d**) as well as 4-[((*E*)-1-{2-hydroxy-5-[(*E*)-2-(aryl)-1-diazenyl]phenyl}methylidene)amino]benzoic acids (**3a**–**d**) are reported. UV–VIS results point towards both azo–hydrazone as well as acid–base equilibrium for the synthesized compounds and solvent plays an important role in determining the predominant species. The structural properties of the compounds were also described by density functional theory (DFT) using B3LYP/6-31g(d) methodology. The theoretical results are in reasonably good agreement with the experimental values. Quantum chemical calculations demonstrated clearly that, the molecules of compounds **2a**–**d** are planar and the loss of planarity was observed in the corresponding compounds **3a**–**d**. In the latter, the precursor part of the molecule remains planar, but the phenyl ring containing the carboxylic (–COOH) group does not belong to the same plain. Compounds **3a**–**d** are presently under preliminary investigation as new metal complexing agents and their performance will be reported in due course.

Acknowledgements

The financial support of the Department of Science & Technology, New Delhi, India (Grant Nos. SR/S1/IC-03/2005, TSBB; SR/S1/PC-13/2005, AKC; SR/FTP/CS-38/2004, SM) and the University Grants Commission, New Delhi, India through SAP-DSA, Phase-III is gratefully acknowledged.

Appendix. Supplementary data

Supplementary data associated with this article can be found in the online version, at doi:10.1016/j.dyepig.2009.02.012.

References

[1] Maley LE, Mellor DP. Nature 1947;159:370.
[2] Calvin M, Wilson KW. Journal of American Chemical Society 1945;67:2003–7.
[3] Vartak DG, Menon KR. Journal of Inorganic and Nuclear Chemistry 1969;31:3141–7.
[4] Mohan Das PN, Trivedi CP. Journal of Indian Chemical Society 1972;49:739–40.
[5] Deshmukh KG, Bhobe RA. Current Science (India) 1977;46:67–9.
[6] Deshmukh KG, Bhobe RA. Journal of Indian Chemical Society 1977;54:375–7.
[7] Khandar AA, Rezvani Z. Polyhedron 1998;18:129–33.
[8] Deshmukh KG, Bhobe RA. Journal of Inorganic and Nuclear Chemistry 1978;40:135–6.
[9] Pardeshi L, Rasheed A, Bhobe RA. Journal of Indian Chemical Society 1980;57:388–90.
[10] Sarma KK, Basu Baul TS, Mishra DD. Synthesis and Reactivity in Inorganic and Metal-Organic Chemistry 1993;23:1277–84.
[11] Sarma KK, Basu Baul TS, Rivarola E, Agrawal RP. Polyhedron 1994;13:2217–22.
[12] Pujar MA, Bharamagoudar TD. Journal of Indian Chemical Society 1980;57:462–5.
[13] Khandar AA, Nejati K. Polyhedron 2000;19:607–13.
[14] Basu Baul TS, Singh KS, Holčapek M, Jirásko R, Rivarola E, Linden A. Journal of Organometallic Chemistry 2005;690:4232–42.
[15] Linden A, Basu Baul TS, Singh KS. Acta Crystallographica Section E 2006;62:o2566–8.
[16] Butcher RJ, Basu Baul TS, Singh KS, Smith FE. Acta Crystallographica Section E 2005;61:o1007–9.
[17] Basu Baul TS, Singh KS, Song X, Zapata A, Eng G, Lyčka A, et al. Journal of Organometallic Chemistry 2004;689:4702–11.
[18] Basu Baul TS, Singh KS, Holčapek M, Jirásko R, Linden A, Song X, et al. Applied Organometallic Chemistry 2005;19:935–44.
[19] Linden A, Basu Baul TS, Singh KS. Acta Crystallographica Section E 2005;61:m2711–3.
[20] Basu Baul TS, Rynjah W, Singh KS, Pellerito C, D'Agati P, Pellerito L. Applied Organometallic Chemistry 2005;19:1189–95.
[21] Němcová I, Čermáková L, Gasparič J. Spectrophotometric reactions. CRC Press; 1996 [chapter 2].
[22] Grabowska A, Kownacki K, Kaczmarek L. Journal of Luminescence 1994;60/61:886–90.
[23] Mitra S, Tamai N. Chemical Physics Letters 1998;282:391–7.
[24] Mitra S, Tamai N. Physical Chemistry Chemical Physics 2003;5:4647–52.
[25] Kletski M, Milov A, Metelisa A, Knyazhansky M. Journal of Photochemistry and Photobiology A: Chemistry 1997;110:267–70.
[26] Zgierski M, Grabowska A. Journal of Chemical Physics 2000;113:7845–52.
[27] Sarma K, Basu Baul TS, Basaiawmoit WL, Saran R. Spectrochimica Acta Part A 1993;49:1027.
[28] Goncharuk VV, Gorchev VF, Chernega AN. Theoretical and Experimental Chemistry 1981;16:330–2.
[29] Ball P, Nicols CH. Dyes and Pigments 1982;3:5–26.
[30] Stoyanov S, Antonov L. Dyes and Pigments 1995;27:133–42.
[31] Joshi H, Kamounah FS, Gooijer C, van der Zwan G, Antonov L. Journal of Photochemistry and Photobiology A: Chemistry 2002;152:183–91.
[32] Lee C, Yang W, Parr RG. Physical Reviews 1988;37B:785–9.
[33] Andersson MP, Uvdal P. Journal of Physical Chemistry Part A 2005;109:2937–41.
[34] Tanabe S, Ebata T, Fujii M, Mikami N. Journal of Chemical Physics 1996;105:408–19.